Strong electrical magnetochiral anisotropy in tellurium

G. L. J. A. Rikken
Laboratoire National des Champs Magnétiques Intenses, UPR 3228 CNRS/EMFL/INSA/UGA/UPS, Toulouse and Grenoble, France

N. Avarvari
MOLTECH-Anjou, UMR 6200, CNRS, Université Angers, 2 Boulevard Lavoisier, 49045 Angers Cedex, France

(Received 18 March 2019; revised manuscript received 13 May 2019; published 27 June 2019)

We report the experimental observation of strong electrical magnetochiral anisotropy in trigonal tellurium (t-Te) crystals. We introduce the tensorial character of the effect and determine several tensor elements. We present a simple model based on the band structure of t-Te and the Boltzmann relaxation time approximation which gives a reasonable description of the principal results.

DOI: 10.1103/PhysRevB.99.245153

I. INTRODUCTION

Chirality is important in many areas of physics, chemistry, and biology, where objects or materials can exist in two nonsuperimposable forms, one being the mirror image of the other (enantiomers). Such a system is not invariant under parity reversal. If in addition it is not invariant under time reversal because it has a magnetization, an entire class of effects called magnetochiral anisotropy (MChA) becomes allowed. The existence of MChA in the optical properties of chiral systems under a magnetic field has been predicted since 1962 [1–5]. It corresponds to a difference in the absorption and refraction of unpolarized light propagating parallel or antiparallel to the magnetic field in a chiral medium. After its first experimental observations [6–8], its existence was confirmed across the entire electromagnetic spectrum, from microwaves [9] to x rays [10].

The existence of MChA was further generalized to other transport phenomena [11]. It was experimentally observed in the electrical transport in bismuth helices [11], carbon nanotubes [12,13], and bulk organic conductors [14], as an electrical resistance R that depends on the handedness of the conductor, and on the relative orientation of electrical current $\mathbf{I}$ and magnetic field $\mathbf{B}$,

$$R^{D/L}(\mathbf{B},\mathbf{I}) = R_0(1+\mu^2 B^2 + \gamma^{D/L}\mathbf{B}\cdot\mathbf{I}),$$

with $\gamma^D = -\gamma^L$ referring to the right- and left-handed enantiomer of the conductor. More recently, such electrical MChA (eMChA) was also observed in chiral magnetic systems [15], [16,17], where it allowed us to study the chiral magnetic order and spin fluctuations. The spin filter effect [18] can also be regarded as a form of eMChA. As another generalization, MChA was very recently observed in the propagation of ultrasound [19]. Although the characteristics of eMChA make it interesting for applications, the small values reported so far have discouraged their development.

Here, we report much larger values for trigonal tellurium (t-Te), and develop a simple model that allows us to identify the principal factors governing the strength of eMChA. Whereas a detailed microscopic theory exists for optical MChA [5], apart from some simplified model calculations [20], a quantitative theory is lacking for eMChA in bulk materials. To stimulate the development of such a theory, we present here the experimental observations of eMChA in t-Te, a simple and well-characterized bulk chiral conductor. The t-Te is a direct gap semiconductor ($E_g = 0.33$ eV), with its conduction band minimum and valence band maximum at the H point in the Brillouin zone. It is intrinsic and nondegenerate at room temperature with a carrier density N around 10^{22} m^{-3}. Its crystal structure consists of parallel stacked helices of three Te atoms per turn (Fig. 1) and belongs to the crystal class 32.

The chirality of t-Te and the absence of time-reversal symmetry at the H point allow for the existence of linear $\mathbf{k}$ terms in the band structure ($\mathbf{k}$ = wave vector) [21]. Using this band structure, several chiroptical properties (see Ref. [22] and references therein) and magneto-optical properties (see Ref. [23] and references therein) of t-Te have been calculated, in good agreement with experiment. The existence of strong eMChA in t-Te is plausible because of its helical crystal structure, and it is further supported by the recent observation of current-induced shifts in the ^{125}Te NMR frequency in t-Te [24]. This observation confirms the existence of strong inverse eMChA in in this material. This effect corresponds to a current-induced longitudinal magnetization present in all chiral conductors [11], and therefore implies the existence of a strong eMChA in t-Te. Theoretical work has addressed several contributions to the inverse eMChA in t-Te (see Ref. [25] and references therein) but cannot be straightforwardly adapted to make quantitative predictions for the direct eMChA effect.

II. EXPERIMENTAL

Single crystals of zone-refined t-Te (purity better than 99.9999%) were commercially obtained [26]. They can be easily cleaved along the c axis, and etching the cleavage surface with hot concentrated sulfuric acid reveals characteristic etch pits from which the crystal axis orientation and the crystal

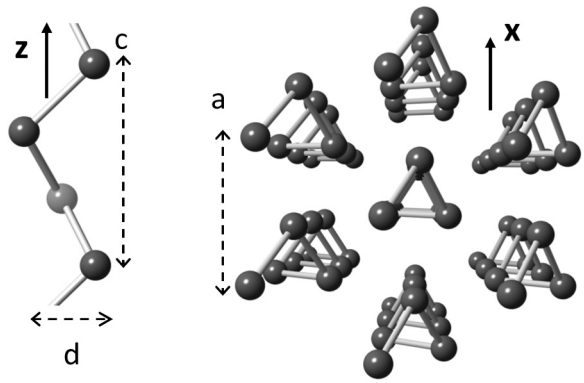

FIG. 1. Trigonal tellurium crystal structure. Left: View on the x-z plane of a single helix. Right: View on the x-y plane. $a = 445$ pm, $c = 593$ pm, $d = 238$ pm.

handedness can be straightforwardly deduced [27]. Typical sample sizes are cross sections of 0.5×0.5 mm^2 and lengths of 4 mm. Gold contacts for collinear four-terminal resistance measurements were deposited by sputtering and a 200-Hz ac current I^ω was injected with a low-distortion current source. The generated voltages V^ω and its second harmonic $V^{2\omega}$ were measured by phase-sensitive detection.

The above expression for $R^{D/L}$ is a simplification, only strictly valid in cubic crystals or isotropic media. In crystals of lower symmetry, the correct description of eMChA requires a fourth rank tensor γ,

$$E_i^{2\omega} = \gamma_{ijkl}^{D/L} J_j^\omega J_k^\omega B_l, \tag{1}$$

where $\gamma_{ijkl}^D = -\gamma_{ijkl}^L$ and J is the current density. The crystal symmetry imposes further restrictions on the tensor components (see, e.g., Ref. [28]).

In the geometry used in our experiments, $i = j = k$, and the cases for $i = x$ and $i = z$ have been addressed by using crystals of different cuts. It can be easily shown that eMChA, defined as $[R(B, I) - R(B, -I)]/[R(B, I) + R(B, -I)] \equiv \Delta R/R$, equals $4V^{2\omega}/V^\omega$ [14]. By taking the difference between the results for $+B$ and $-B$, all nonlinearities that are even in the magnetic field are eliminated. The dependence of $\Delta R/R$ on current and magnetic field for an x-oriented left-handed crystal (space group D_3^6) is shown in Fig. 2, confirming the strictly linear dependence of eMChA on these quantities. By making different crystal cuts and by rotating the crystals, different tensor components can be measured, as illustrated in Figs. 3 and 4.

The enantioselectivity of the eMChA is illustrated in Fig. 4, which shows eMChA results for a left-handed and a right-handed crystal (space group D_3^4) in the same orientation, with opposite results.

From Figs. 3 and 4 we deduce $3\gamma_{xxxx} \approx \gamma_{xxyy}$, $12\gamma_{zzzx} \approx \gamma_{xxyy}$, and $\gamma_{zzzz} \ll \gamma_{zzzx}$. The latter result does not mean that $\gamma_{zzzz} = 0$, as there is no symmetry argument that imposes that. The uncertainty in the exact geometrical shape of the sample, in combination with the small value of γ_{zzzz} and the much larger values of the other tensor elements, make it difficult to determine a significant value for this quantity. Figure 5 shows the temperature dependence of eMChA in the intrinsic regime around room temperature.

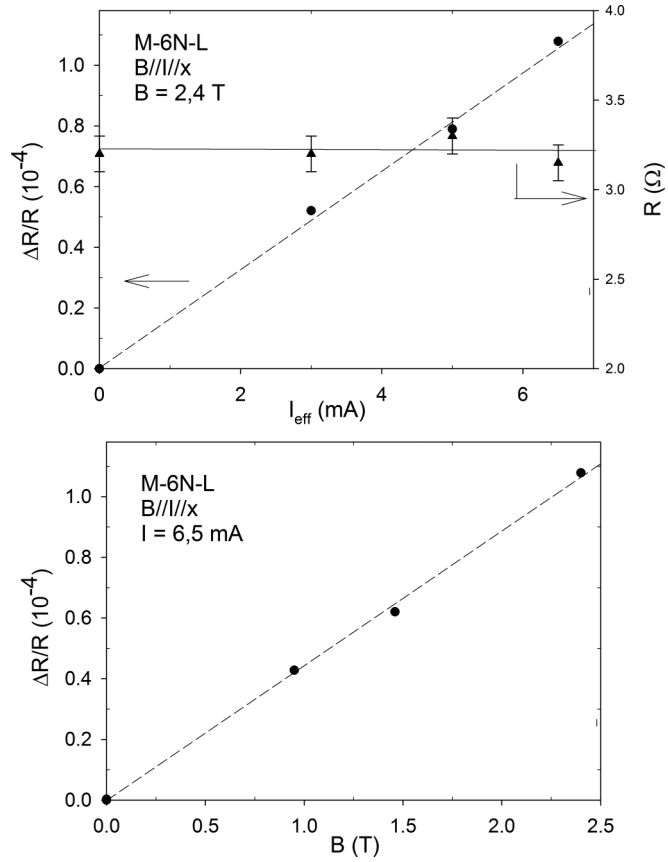

FIG. 2. Current and magnetic field dependence of the eMChA of an x-oriented left-handed Te crystal at room temperature. The sample cross section is 5×10^{-7} m^2.

III. DISCUSSION

Table I gives a summary of the values reported so far for eMChA, illustrating that t-Te shows by far the strongest effect. The explanation for the observed eMChA tensor components

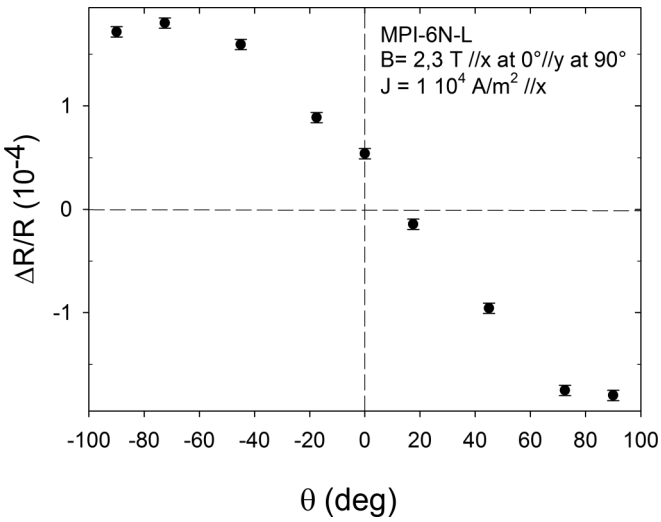

FIG. 3. eMChA of an x-oriented left-handed crystal at room temperature, as a function of the angle between **B** and the crystal x axis. At $\theta = 0°$, $\Delta R/R \propto \gamma_{xxxx}$, and at $\theta = \pm 90°$, $\Delta R/R \propto \gamma_{xxyy}$.

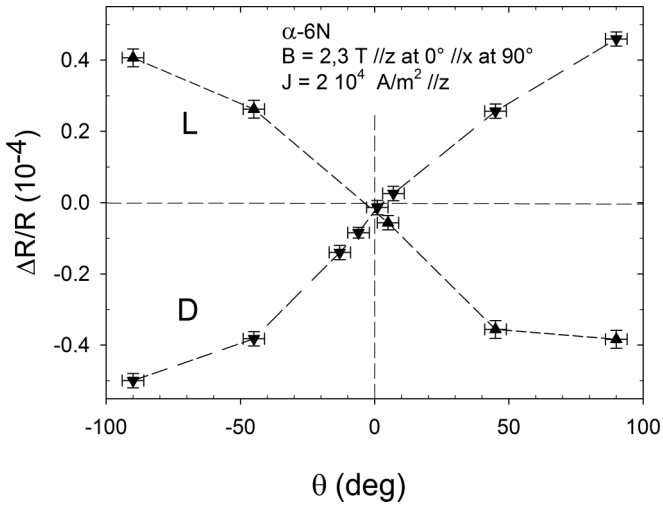

FIG. 4. eMChA of a left-handed (▲) and right-handed (▼) z-oriented Te crystal at room temperature, as a function of the angle between $\mathbf{B}$ and the crystal z axis. At $\theta = 0°$, $\Delta R/R \propto \gamma_{zzzz}$, and at $\theta = \pm 90°$, $\Delta R/R \propto \gamma_{zzzx}$.

lies in the $\mathbf{k}$-linear terms in the t-Te band structure around the H point. Nakoa *et al.* [29] have shown theoretically and experimentally that these terms lead to the lifting of the energy degeneracy between valence band states with $\mathbf{k}$ and $-\mathbf{k}$ in the presence of a magnetic field perpendicular to the z axis, whereas no degeneracy lifting occurs for a magnetic field parallel to the z axis. Although the authors did not comment on this aspect, such an energy splitting has to be enantioselective in order to be symmetry allowed. We can therefore heuristically simplify their findings to the existence of a MChA energy term around the t-Te valence band maximum of the form $\Delta\epsilon_v = \chi^{D/L}\mathbf{k}\cdot\mathbf{B}_\perp$, with $\chi^D = -\chi^L$ and $|\chi| = 1.5 \times 10^{-30}$ J m/T. A similar behavior was later found for the t-Te conduction band [30]. If we neglect the regular nonparabolicity of the valence band, its energy dispersion relation around the H point is $\epsilon(\mathbf{k}) = \hbar^2\mathbf{k}^2/2m^* + \chi^{D/L}\mathbf{k}\cdot\mathbf{B}_\perp$. In the constant relaxation time approximation,

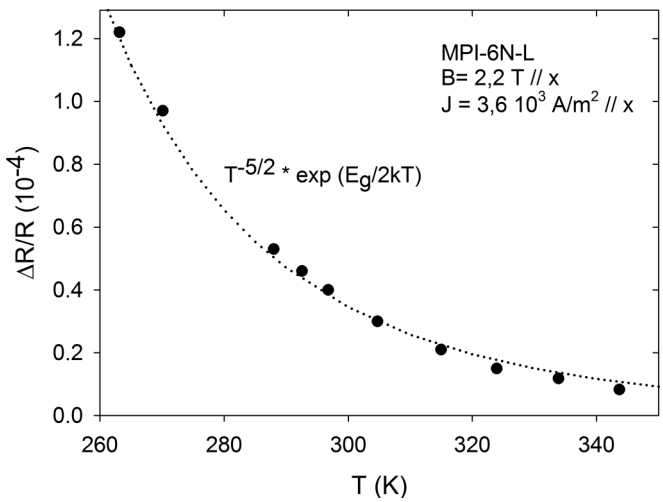

FIG. 5. Temperature dependence of eMChA of an x-oriented left-handed crystal. For the dotted line, see text.

TABLE I. Summary of published eMChA results (RT: room temperature; LT: low temperature; SWCNT: single-wall carbon nanotube; TTF-ClO_4: dimethyl-ethylenedithio-tetrathiafulvalene perchlorate.)

Material	γ (m^2/T A)	Ref.	Remark
t-Te $xxxy$	10^{-8}	This work	RT
TTF-ClO_4	10^{-10}	[14]	RT
$CrNb_3S_6$	10^{-12}	[17]	Magnetic, LT
MnSi	2×10^{-13}	[15]	Magnetic, LT
SWCNT	10^{-14}	[12]	LT

the Boltzmann equation gives for the electrical conductivity σ [31],

$$\sigma_{ii} = \frac{q^2\tau}{4\pi^3\hbar^2}\int\left(\frac{\partial\epsilon(\mathbf{k})}{\partial k_i}\right)^2\frac{\partial f}{\partial\epsilon}d^3\mathbf{k}, \tag{2}$$

where f is the distribution function, q the charge, τ the scattering time, m^* the effective mass, and for Maxwell-Boltzmann statistics, $\partial f/\partial\epsilon = -f/k_BT$. Applying the magnetic field in the x direction and neglecting terms in B^2, this results in

$$\sigma_{xx} = \frac{Nq^2\tau}{m^*} - \frac{q^2\tau\chi^{D/L}B}{4\pi^3 m^* k_B T}\int k_x f d^3\mathbf{k} \tag{3}$$

$$= \sigma_0\left(1 - \gamma^{D/L}_{xxxx}J_xB\right), \tag{4}$$

where

$$\gamma^{D/L}_{xxxx} = m^*\chi^{D/L}/Nq\hbar k_BT. \tag{5}$$

Note that at room temperature an analogous contribution to eMChA will come from the conduction band which, depending on the relative signs of χ for the two bands, may have the same or opposite sign. This electron contribution will disappear at low temperature when t-Te becomes extrinsically p type. This simple model leads to several predictions:

(1) As a general rule, metals, with their much larger carrier density, will show a smaller eMChA than semiconductors and semimetals, in agreement with the table above.

(2) For t-Te at 300 K, $\Delta R/R(\mathbf{B} \parallel \mathbf{J} \parallel \mathbf{x}) = \gamma_{xxxx}JB$, with $\gamma_{xxxx} \approx 6 \times 10^{-10}$m^2 A^{-1} T^{-1}, whereas our experimental result (Fig. 3) gives $\gamma_{xxxx} \approx 2 \times 10^{-9}$ m^2 A^{-1} T^{-1}, a reasonable agreement in view of the simple model.

(3) $\gamma_{iiiz} = 0$ in t-Te because of the absence of the degeneracy lifting for $\mathbf{B} \parallel \mathbf{z}$, in agreement with our observations. Other mechanisms for eMChA [11], not included in our model, may still lead to a small nonzero value. One may obtain an estimate for γ_{zzzz} from the free-electron-on-a-helix model [20]. This can only give an upper limit, as there is significant coupling between adjacent Te helices and charge carriers are therefore not confined to one helix. For the same parameters as in Fig. 4, this model predicts $\Delta R/R \approx 10^{-9}$, consistent with the experimental result.

(4) Taking into account the temperature dependence of the carrier concentration [31], Eq. (5) implies the temperature dependence of γ_{xxxx} to be $T^{-5/2}\exp(E_g/2k_BT)$. Figure 5 shows that this is a reasonably good description. Although t-Te is topologically trivial, the existence of $\mathbf{k}$-linear terms in its band structure and its strong spin-orbit interaction suggest

a link to topological insulators and Weyl semimetals. Indeed, strong eMChA was also claimed for topologically nontrivial systems such as Weyl semimetals [32] and noncentrosymmetric Rashba superconductors [33], although these systems are not chiral in the strict sense of the term. In line with this suggestion, *t*-Te is predicted to become a strong topological insulator under pressure [34] and angle-resolved photoemission spectroscopy (ARPES) measurements have revealed Weyl nodes at ambient pressure [35].

It will be clear that a more sophisticated theoretical approach, including the effect of the Lorentz force, plus the full details of the band structure are necessary to obtain a fuller understanding of eMChA in *t*-Te and to arrive at an accurate description of all its tensor elements. Our simple model allows us to identify the major contributing factors and will help to identify other materials that could show strong eMChA, thereby opening a venue for realistic applications of this effect. Obvious candidates are trigonal selenium and its binary alloys with tellurium, and cinnabar (α-HgS) that have the same crystal structure, albeit slightly different band structures. At different band-structure extrema, the MChA energy term, present around the *H* point in *t*-Te, may be zero because of crystal symmetry, which could lead to a much lower eMChA.

In summary, we have experimentally observed strong eMChA in trigonal tellurium, we have demonstrated the tensorial character of this effect, and we have developed a simple model that allows us to qualitatively understand two of its diagonal tensor elements.

ACKNOWLEDGMENT

This work was supported by the Agence Nationale de la Recherche (ChiraMolCo, No. ANR 15-CE29-0006-02).

[1] M. P. Groenewege, Mol. Phys. **5**, 541 (1962).
[2] D. L. Portigal and E. Burstein, J. Phys. Chem. Solids **32**, 603 (1971).
[3] N. B. Baranova, Yu. V. Bogdanov, and B. Ya. Zeldovich, Opt. Commun. **22**, 243 (1977).
[4] G. Wagnière and A. Meier, Chem. Phys. Lett. **93**, 78 (1982).
[5] L. D. Barron and J. Vrbancich, Mol. Phys. **51**, 715 (1984).
[6] G. L. J. A. Rikken and E. Raupach, Nature (London) **390**, 493 (1997).
[7] P. Kleindienst and G. Wagnière, Chem. Phys. Lett. **288**, 89 (1998).
[8] G. L. J. A. Rikken and E. Raupach, Phys. Rev. E **58**, 5081 (1998).
[9] S. Tomita, K. Sawada, A. Porokhnyuk, and T. Ueda, Phys. Rev. Lett. **113**, 235501 (2014); Y. Okamura, F. Kagawa, S. Seki, M. Kubota, M. Kawasaki, and Y. Tokura, *ibid.* **114**, 197202 (2015).
[10] M. Ceolín, S. Goberna-Ferrón, and J. R. Galán-Mascarós, Adv. Mater. **24**, 3120 (2012); R. Sessoli, M. Boulon, A. Caneschi, M. Mannini, L. Poggini, F. Wilhelm, and A. Rogalev, Nat. Phys. **11**, 69 (2015).
[11] G. L. J. A. Rikken, J. Fölling, and P. Wyder, Phys. Rev. Lett. **87**, 236602 (2001).
[12] V. Krstić, S. Roth, M. Burghard, K. Kern and G. L. J. A. Rikken, J. Chem. Phys. **117**, 11315 (2002).
[13] J. Wei, M. Shimogawa, Z. Wang, I. Radu, R. Dormaier, and D. H. Cobden, Phys. Rev. Lett. **95**, 256601 (2005).
[14] F. Pop, P. Auban-Senzier, E. Canadell, G. L. J. A. Rikken, and N. Avarvari, Nat. Commun. **5**, 3757 (2014).
[15] T. Yokouchi, N. Kanazawa, A. Kikkawa, D. Morikawa, K. Shibata, T. Arima, Y. Taguchi, F. Kagawa, and Y. Tokura, Nat. Commun. **8**, 866 (2017).
[16] H. Maurenbrecher, J. Mendil, G. Chatzipirpiridis, M. Mattmann, S. Pané, B. J. Nelson, and P. Gambardella, Appl. Phys. Lett. **112**, 242401 (2018).
[17] R. Aoki, Y. Kousaka and Y. Togawa, Phys. Rev. Lett. **122**, 057206 (2019).
[18] R. Naaman and D. H. Waldeck, Annu. Rev. Phys. Chem. **66**, 263 (2015).
[19] T. Nomura, X.-X. Zhang, S. Zherlitsyn, J. Wosnitza, Y. Tokura, N. Nagaosa, and S. Seki, Phys. Rev. Lett. **122**, 145901 (2019)
[20] V. Krstić and G. L. J. A. Rikken, Chem. Phys. Lett. **364**, 51 (2002).
[21] T. Doi, K. Nakao, and H. Kamimura, J. Phys. Soc. Jpn. **28**, 36 (1970).
[22] S. S. Tsirkin, P. A. Puente, and I. Souza, Phys. Rev. B **97**, 035158 (2018).
[23] *The Physics of Selenium and Tellurium*, edited by E. Gerland and P. Grosse (Springer, Berlin, 1979).
[24] T. Furukawa, Y. Shimokawa, K. Kobayashi, and T. Itou, Nat. Commun. **8**, 954 (2017).
[25] C. Şahin, J. Rou, J. Ma, and D. A. Pesin, Phys. Rev. B **97**, 205206 (2018).
[26] Alfa Aesar catalog No. 11076.
[27] A. Koma, E. Takimoto, and S. Tanaka, Phys. Status Solidi **40**, 239 (1970).
[28] R. R. Birss, *Symmetry and Magnetism* (North-Holland, Amsterdam, 1966).
[29] K. Nakao, T. Doi, and H. Kamimura, J. Phys. Soc. Jpn. **30**, 1400 (1971).
[30] J. Blinowski, G. Rebmann, C. Rigaux, and C. Mysielskci, J. Phys. (Paris) **38**, 1139 (1977).
[31] K. H. Seeger, *Semiconductor Physics* (Springer, Berlin, 1982).
[32] T. Morimoto and N. Nagaosa, Phys. Rev. Lett. **117**, 146603 (2016).
[33] R. Wakatsuki, Y. Saito, S. Hoshino, Y. Itahashi, T. Ideue, M. Ezawa1, Y. Iwasa and N. Nagaosa, Sci. Adv. **3**, e1602390 (2017).
[34] L. A. Agapito, N. Kioussis, W. A. Goddard, III, and N. P. Ong, Phys. Rev. Lett. **110**, 176401 (2013).
[35] K. Nakayama, M. Kuno, K. Yamauchi, S. Souma, K. Sugawara, T. Oguchi, T. Sato, and T. Takahashi, Phys. Rev. B **95**, 125204 (2017).